Construction and Building Materials 262 (2020) 120095

Contents lists available at ScienceDirect

Construction and Building Materials

journal homepage: www.elsevier.com/locate/conbuildmat

FT-IR study of early stages of alkali activated materials based on pyroclastic deposits (Mt. Etna, Sicily, Italy) using two different alkaline solutions

Claudio Finocchiaro [a], Germana Barone [a], Paolo Mazzoleni [a,*], Cristina Leonelli [b], Ameni Gharzouni [c], Sylvie Rossignol [c]

[a] Dipartimento di Scienze Biologiche, Geologiche e Ambientali, Università di Catania, Corso Italia, 57, Catania, 95127 Sicily, Italy
[b] Dipartimento di Ingegneria "Enzo Ferrari", Università di Modena e Reggio Emilia, Via Pietro Vivarelli 10, 41125 Modena, Italy
[c] IRCER (Institut de Recherche sur les Céramiques), University of Limoges, 12, Rue Atlantis, 87100 Limoges, France

HIGHLIGHTS

- Binary mixtures with pyroclastic deposits (Mt. Etna volcano) and metakaolin.
- Alkaline activating solutions based on Na or K cation.
- Polycondensation reaction monitoring on fresh pastes through *In situ FTIR* analysis.
- Performance in terms of structure, compressive strengths and porosity.

GRAPHICAL ABSTRACT

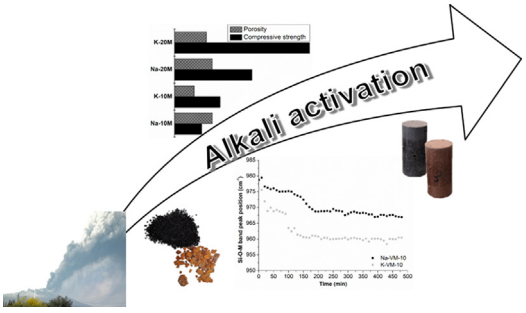

ARTICLE INFO

Article history:
Received 19 April 2020
Received in revised form 25 June 2020
Accepted 26 June 2020

Keywords:
Geopolymer
FTIR spectroscopy
Volcanic ash
Polycondensation reaction
Na and K-silicates
Mechanical properties

ABSTRACT

The huge availability of volcanic deposits in Mt. Etna volcano and the wide use of volcanic materials as aggregates in local architecture encouraged us to apply them in alkaline environment to produce geopolymeric binders to restore historical buildings of Mt. Etna area. Two clusters of samples for each volcanic precursor (volcanic ash and ghiara paleo-soil) were produced, using 10 and 20% wt. of metakaolin and two different alkaline solutions based on sodium and potassium respectively. A comparative study was made in relation to activators used, focusing on evaluation of polycondensation step (in ATR); chemical and structural characterization (FT-IR); TGA analysis, qualitative XRD analysis and mechanical compressive test after 7 and 21 curing days. ATR results confirmed the occurrence of geopolymerization for all samples; FT-IR analysis showed a higher content of carbonates in potassium-samples, decreasing at increasing of metakaolin content. A low weight lost was recorded in consolidated samples, as well as a partial dissolution of volcanic phases. Higher mechanical compressive strengths for K-samples, reaching 89 MPa as highest value after 21 days, differently to sodium-samples (51 MPa) were recorded, reflecting the porosity of the different specimens.

1. Introduction

The interest to develop new construction materials which are environmentally friendly, low-energy-consuming and cost-efficient, as well as the attention to a sustainable management of

* Corresponding author.
E-mail address: paolo.mazzoleni@unict.it (P. Mazzoleni).

https://doi.org/10.1016/j.conbuildmat.2020.120095
0950-0618/

waste materials, increased exponentially in the last decades [1–3]. In this scenario, geopolymer and alkali activated materials (AAMs) are good alternatives, enclosing all features requested by industrial community. These materials are produced by the activation of an aluminosilicate source with an alkaline solution [4,5]. The chemical reaction includes different steps starting from the dissolution of aluminosilicate precursors activated by an alkaline solution to a polycondensation reaction, forming an amorphous three-dimensional network. However, the recognition of each reaction steps is very complicated due to their contemporary and rapid manifestation [6] and also because they are strongly dependent with raw material type, becoming difficult to propose a single reaction kinetics model.

Volcanic precursor is one of the most suitable aluminosilicate source for AAMs production thanks to high amorphous content generated by the rapid quenching during a volcanic explosion which prevail on crystallinity grade, as well as different oxides contents compared to SiO_2/Al_2O_3 [7–9]. However, volcanic glass maintains higher stability in alkaline environment in comparison with other more common precursors, such as metakaolin and fly ashes, requiring thermal treatments to enhance the final properties of AAM as proposed in literature (e.g. [10]). In this context, Mt. Etna materials represent an important resource that may be exploited as raw material aluminosilicate sources for AAMs production, although thermal treatments or metakaolin addition (10–25%) was required to reduce the setting time [11]. Mt. Etna volcano, located in the bigger island of Italy (Sicily), is the second most active volcano in the world, following the Kilauea volcano on Hawaii and preceding the Piton de la Fournaise on La Réunion island. However, it preserves the Guinness as Europe's highest volcano. Behind the volcano activity, a potential risk is linked to the volcanic ash emissions. Moreover, volcanic ash, once erupted, represents a waste material due to the possible interactions with other anthropic and environment matrixes, representing so a serious management problem. Various attempts were tried to use the products of recent eruption as aggregates in traditional mortar production, taking into account the weight ratios of aggregates/binder, grain size of aggregates and thus their destination of use [12]. However, the ashes interaction with the volcanic gasses represents an important limit due to the negative effects of the high chlorides and sulphates deposited on the particles surface [13]. Contrary, old pyroclastic deposits in which the undesirable elements had been leached, are largely used in the traditional cement industry. Moreover, Mt. Etna volcano, in addition to the common massive and pyroclastic rocks, offers another volcanic material, locally named *ghiara*. It is a volcanic paleo-soil generated by high temperature and oxidizing conditions reached in contact with the overlying lava flow, to which it owes its uniqueness in the world [11]. The addition of *ghiara* in the plasters and mortars as aggregate was a common practice in the seventeen and eighteen centuries in this area of Sicily due to its peculiar reddish hue and high hydraulic modulus [14–19].

In this work, volcanic materials of Mt. Etna volcano, specifically volcanic ash and ghiara paleo-soil, were activated using two type of alkaline solutions: i) sodium-based, developed at Dept. of Biological, Geological and Environmental Sciences (Catania University); ii) potassium-based, provided by IRCER lab (Limoges University). Formulations developed using these two different activators were compared with the goal of highlighting the strengths and weaknesses in terms of polycondensation rate, structure and mechanical strengths. In detail, in situ *FTIR* and TGA analyses were aimed to evaluate the development of molecular reticulation, while XRD analysis the dissolution of crystalline phases, as well as mercury intrusion porosimetry (MIP) and mechanical test for porosity and compressive strength, respectively.

2. Experimental part

2.1. Raw materials

In this work, volcanic ash, considering with this term all the pyroclastic rocks with dimension <64 mm, was sampled near Santa Venerina, Italy, a small town in the south-east slope of Mt. Etna volcano, following the 16 March 2013 eruption. A first grain size selection was made sieving the deposit, choosing the <2 mm fraction. The particles have been cleaned with water after the sampling to remove organic elements. Ghiara deposit were sampled in the "Orcio" quarry, situated in the area of Trecastagni village (in the south slope of Mt. Etna). Historically, it was widely used for ghiara extraction due to its large extension, representing one of the most important anthropic cavities of Etnean area. The thick of this deposit is variable (1.20–1.60 m), mainly characterized by a grain size between 2 mm and 0.5 mm. Ghiara colour changes tones from yellowish to reddish ones according to the layer position respect the lava roof.

Once the moisture has dried and removed at 110 °C using an oven, both materials were dry milled (using porcelain jars and alumina balls after sediment quartering). In detail, volcanic ash was milled, following a preliminary and manually sieving, starting from 500 μm (d90) for 1 h, while ghiara starting from 120 μm (d90) for 45 min, until to reach a grain size quite homogeneous in comparison to commercial metakaolin.

The chemical molar ratios of volcanic precursors and metakaolin, used as additive to enhance the reactivity of the system and whose chemical composition provided by Balco company, have been listed in Table 1. For each volcanic raw materials, four alkaline activations were carried out using the addition of 10 and 20% wt. (on the total weight of the powder) of metakaolin, known as ARGICAL™ M1000 [20], (IMERYS, France, reported chemical composition from producer: SiO_2 = 55%; Al_2O_3 = 40%, Fe_2O_3 = 1.4%; TiO_2 = 1.5%; $Na_2O + K_2O$ = 0.8%; CaO + MgO = 0.3%; LOI = 1%), and two different alkaline activators based on Na or K alkaline cation.

2.2. Samples preparation

For the Na solution, combination of sodium hydroxide (8 M) and sodium silicate, provided by Ingessil s.r.l. with a molar ratio SiO_2/Na_2O = 3 was used, while a potassium silicate, commercially named Geosil 14515, provided by Wollner with 0.65Si/K molar ratio [21], were used for the K solution. The same formulation protocol was used: preparation of solutions and following addition of the powders, once weighted in a precision balance; mixing with mechanical mixer for 5 min and, once filled the cylindrical plastic pots, vibrating to remove air bubbles. High viscosity was obtained for every formulation with a liquid / solid (L/S) ratio ~0.3 to reduce at minimum the use of alkaline solution and the setting time. Four samples for each volcanic precursor (indicating with the letter "V",

Table 1
Chemical molar ratio of raw materials (volcanic ash, ghiara raw and metakaolin) used as precursors in alkaline activation.

Ratios	*Volcanic ash raw*	*Ghiara raw*	*Metakaolin*
Si/Al	2.54	2.17	1.17
Si/Fe	5.56	5.50	52.21
Si/Mg	8.27	11.90	–
Si/Ca	4.37	5.90	–
Fe/Al	0.46	0.40	0.02
Mg/Al	0.31	0.18	–
Ca/Al	0.31	0.37	–
LOI	0.44	0.49	1

the samples with volcanic ash, while with the "G", the samples with ghiara) were prepared: two activated by sodium solution (prefix Na-) and likewise the others by potassium (prefix K-) with the respectively of 10 and 20% wt of metakaolin (M−10 or M−20) used as additive to allow the reaction at room temperature, simulating so in situ applications. Therefore, the samples with volcanic ash activated by sodium solution were labeled with Na-VM-10 and Na-VM-20, while those with the potassium one, K-VM-10 and K-VM-20, as well as the samples with ghiara as listed in Table 2.

2.3. Characterization techniques

Several characterization techniques were chosen with the aim to evaluate firstly the polycondensation reaction of the fresh pastes (in situ FTIR analysis) and of the solid geopolymers (FTIR in KBr mode, XRD and TGA analyses), once evaluated the chemical stability in water and at air exposure according the procedure explained in [11]. Additionally, we evaluated the physical–mechanical performance of consolidated materials (through MIP analysis and compressive test). For this latter, ten samples were prepared, whose sherds or their powders were used for the other techniques to obtain a complete characterization of binders. Generally, each measurement was replicated three times.

2.3.1. FT-IR analysis

In this work, two different FT-IR approaches were used. On one hand, punctual and continuous measurements on fresh alkaline pastes to observe the structural changes in time after the alkaline reaction, while on the other hand, measurements on consolidated samples after 21 days. All measurements were performed using a Thermo Fisher Scientific 380 infrared spectrometer (Nicolet). For the first approach, a micro diamond cell was used and punctual analysis were carried out all fresh paste starting from 0 to 8 h recording every 10 min. In detail, once mixed the aluminosilicate sources with both alkaline solutions, a drop of each formulation was deposited onto diamond substrate of FT-IR apparatus in the ATR mode to monitor the structural evolution of the synthesized mixtures. This technique permits to observe two steps: solid mixture dissolution's and the geopolymerization process, thus highlighting the kinetic variations of samples activated respectively with both alkaline solutions. Contrary, KBr method was carried out as second approach. Briefly, pellets were prepared by mixing 1 mg of powdered sample with 150 mg of KBr. The mixture was then compressed with a manual press applying 6 metric-tons of force. For each sample three pellets were prepared to have a good statistical redundancy. All IR spectra, regarding both approaches, were recorded between 4000 and 400 cm^{-1} with a resolution of 4 cm^{-1}. For comparison, the spectra were baseline-corrected and normalized [22] and treated in absorbance. The OMNIC software (Nicolet Instruments) was used for data acquisition and spectral analysis.

Table 2
List of formulations, detailing labels, precursors and activating solutions.

Labels	*Volcanic powder*	*Metakaolin (% wt)*	*Activating solution*
Na-VM-10	Volcanic ash	10	Sodium
Na-GM-10	Ghiara		
Na-VM-20	Volcanic ash	20	
Na-GM-20	Ghiara		
K-VM-10	Volcanic ash	10	Potassium
K-GM-10	Ghiara		
K-VM-20	Volcanic ash	20	
K-GM-20	Ghiara		

2.3.2. XRD analysis

X-ray diffraction (XRD) patterns were obtained with a Brucker-D8 Advance with a Bragg-Brentano geometry and a Cu Kα1α2 detector. The analytical range is between 20 and 50 (2θ) with a resolution of 0.02 (2 θ) and a dwell time of 1.5 s. Phase identification was performed with reference to a Joint Committee Powder Diffraction Standard (JCPDS). The patterns were processed using Eva software.

2.3.3. TGA/TDA analysis

Thermal analysis was performed both on volcanic raw materials as well as on AAMs, aged 7 days, using an SDT-Q600 apparatus from Thermal Analyzer in an atmosphere of flowing dry air (100 mL/min). The signal was measured with Pt/Pt-10% Rh thermocouples. The volcanic precursors were heated at 1350 °C with a rate of 5 °C/min in alumina crucibles under air, while the AAMs were heated at 500 °C with a rate of 5 °C/min using platinum crucibles.

2.3.4. Mechanical compressive test

Compressive test was performed on 5 samples of each formulation, using an Instron 5969 universal testing machine with a cross-head speed of 0.5 mm/min and a 50 kN sensor. The samples were cylindrical in shape with a diameter of 15 mm and a height of approximately 30 mm. Once hardened, respectively at 7 and 21 days, rectification on both basal surfaces were carried out to obtain homogenous and parallel surfaces.

2.3.5. Hg intrusion porosimetry (MIP) test

All consolidated samples were analysed by Hg intrusion porosimetry (MIP) to investigate the porosity at sub-micrometric scale once removed humidity in the oven at 105 °C temperature. In this scenario, shards of specimens activated by both alkali solutions were compared, as well as the influence of volcanic precursors and the amount of metakaolin used as additive were evaluated. Porosimetric analysis was carried out with a Thermoquest Pascal 240 macropore unit in order to explore a porosity range ~0.0074 μm < r < ~15 μm (indicating with r the radius of the pores), and by a Thermoquest Pascal 140 porosimeter instrument in order to investigate a porosity range from ~3.8 μm < r < ~116 μm.

3. Results and discussions

3.1. Raw materials

The chemical composition of the three used precursors (V, G and M) was determined. The molar ratios of the major elements are presented in Table 1. V, G precursors show higher Si/Al molar ratio than metakaolin (2.54, 2.17 and 1.17 for V, G and M respectively). V and G are also rich in iron, magnesium and calcium elements compared to metakaolin. The mineral phases were also determined. XRD patterns are presented in Fig. 4. The crystalline phases present in metakaolin are quartz, anatase and muscovite. However, V and G show more crystalline phases such as anorthite, augite, forsterite, magnetite and hematite with different peak intensities.

Thermal analysis (DTA -TGA) were carried out on raw materials. The obtained thermal curves of volcanic precursors are showed in Fig. 1. Both V and G showed a very low weight loss about 0.5% until 200 °C corresponding to the elimination of physically adsorbed water. Afterwards, the main weight loss was recorded at 500 °C (1%) for volcanic ash (Fig. 1a), whereas at 1100 °C (1%), ending point of analysis, for ghiara (Fig. 1b) following a possible release of silica hydroxyl groups (Si (OH_4))[21]. These low values are in

Table 3
Weight's loss values in the two temperature regions (25–200 °C and 200–500 °C) for all the AAMs considered.

	Ranges (°C)	VM				GM			
		10		20		10		20	
		Na	K	Na	K	Na	K	Na	K
% Weight loss	25–200	7.8	6.2	6.3	7.1	4.9	4.9	6.5	6.1
	200–500	0.6	0.7	0.8	1.0	0.7	0.9	1.0	1.2
	Total	8.3	6.9	7.1	8.1	5.7	5.8	7.5	7.4

Table 4
Values of apparent density and average mechanical compressive strength (MPa) of all samples after 7 and 21 of aging days.

Labels	*After 7 days*		*After 21 days*	
	App. ρ (g/cm³)	*σ (MPa)*	*App. ρ (g/cm³)*	*σ (MPa)*
Na-VM-10	2.155	17	2.150	18
Na-GM-10	2.145	16	2.139	17
Na-VM-20	2.132	44	2.122	50
Na-GM-20	2.129	46	2.124	51
K-VM-10	2.191	23	2.197	29
K-GM-10	2.211	26	2.208	30
K-VM-20	2.176	69	2.161	71
K-GM-20	2.161	78	2.163	89

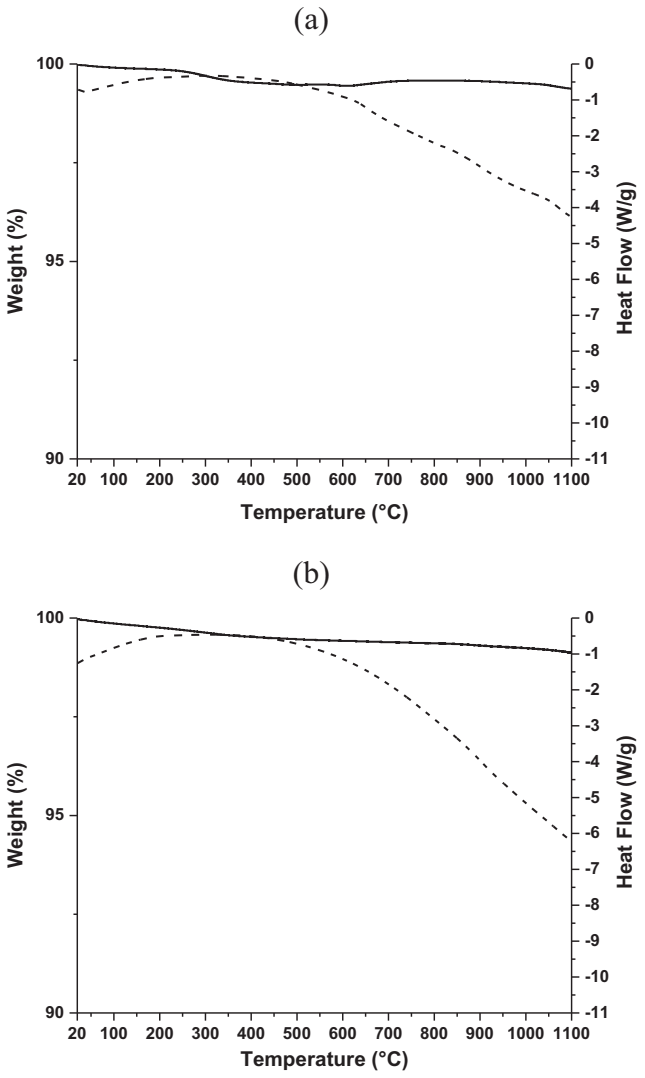

Fig. 1. Thermal analysis curves of weight loss (—) and heat flow (–) for (a) V and (b) G raw materials.

accordance with literature [23,24] and confirmed the volcanic origin of both raw materials, in addition to the further natural oxidation undergone by ghiara during its formation with the covering lava layer such as to require higher temperature before structural modifications occurrence. To corroborate these data, FTIR analysis were performed on volcanic precursors (see Fig. S1 as supplementary files) which revealed only the presence of aluminosilicates species.

According to these results, volcanic precursors show differences compared metakaolin ones, suggesting different reactivity in alkaline environment.

3.2. Fresh geopolymeric pastes

Different samples were synthetized based on Na or K solution with a mixture of volcanic precursors (V and G) and 10 or 20 wt % of metakaolin as detailed in Table 2. The fresh pastes were monitored by in-situ FTIR spectroscopy to record the structural evolution. The main peak position related to Si-O-M band is plotted in function of time in Fig. 2. Whatever the sample, a continuous and progressive shift of the Si-O-M band position in time toward lower wavenumbers was evidenced. This behaviour indicates the substitution of Si–O–Si by Si–O–Al bonds which reflects a polycondensation reaction [22]. Moreover, the slope of the curve is characteristic of the kinetics of this substitution (i.e. low slope indicates a slow kinetic) [25]. Na/K-VM-10/20 showed the same behaviour regardless of the different quantity of metakaolin added in the mixture. In both cases, the trends of the samples, activated with Na solution, highlighted higher wavelengths than that ones with K solution (Fig. 2 a-b). Analogously, Na/K-GM-10/20 showed the same trend. However, differently from Na/K-VM-10/20, the samples with 20% of M showed a higher displacement among the two trends (Fig. 2 d), while a different behaviour was recorded for the samples with 10% of M. In this latter case, the trends, initially, showed the high displacement, which was recovered over time (Fig. 2 c). For all the samples considered regardless the type of volcanic precursors used and the quantity of M added, the shift is almost the same reaching values ranging 12–18 cm^{-1}, as well as the slope of the curves expect for Na/K-GM-10 sample. Therefore, FT-IR analysis in situ on the slurries were useful to demonstrate the occurrences of polycondensation reactions. Moreover, the obtained shift values are characteristic of aluminosilicate network

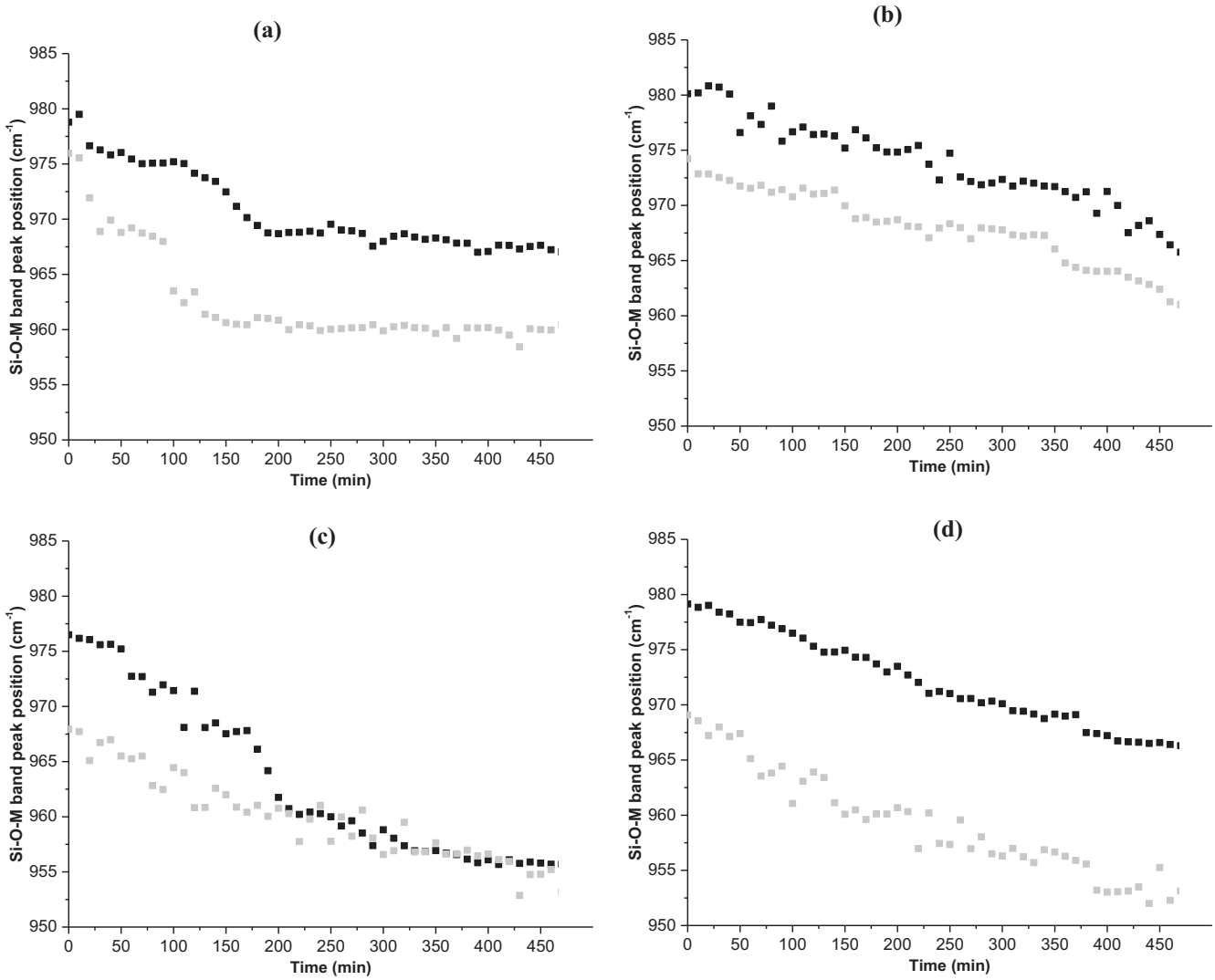

Fig. 2. Trends of FT-IR considering the progressive shift of Si-O-M positions in function of time, for (a) VM-10, (b) VM-20, (c) GM-10 and (d) GM-20, samples activated with sodium solution (■) or with potassium solution (▰).

formation, although are lower than other formulations based on metakaolin [20]. However, to make sure of an exhaustive comprehension of the reaction rate, NMR analysis is necessary.

3.3. Hardened samples

3.3.1. Structural data

All consolidated samples considered in this work were analyzed also using FT-IR with KBr method with the aim to characterize their structures. The results showed for both series (VM and GM) the same behaviour: no differences in terms of water content or silicate contributions. In the first case, vibrations of bound water molecules were recorded at 3445 and 1650 cm^{-1} assigned to the stretching (–OH) and bending (H–O–H) respectively [24,26], while the silicate structure is characterized by the main peak located at 1015 cm^{-1} related to the vibration of SiO/Al–O bond of aluminosilicate framework reflecting the formation of the amorphous aluminosilicate gel in binary systems [27] and by the ring vibrations of Si–O bonds of silicate network at 575 and 530 cm^{-1} [24,26] (Fig. 3a). However, an evident difference in terms of intensity for the influence of carbonates, located at 1430 and 1385 cm^{-1} (Fig. 3b), corresponding to the stretching vibrations of O-C-O bonds in the carbonate group (CO_3^{2-}) due to the carbonation reaction between the carbon dioxide from the air and the geopolymer was recorded [28–31]. The detected increases were caused by a larger carbonation due to high free ions amount. The contribution of carbonates is higher in the samples activated using potassium solution and in those one with 10 wt% of M added revealing the presence of free alkali cation which can react with atmospheric CO_2 to form K_2CO_3 or Na_2CO_3 species [32], while the decreasing of intensity, recorded in samples with higher metakaolin amount can be explained by lower amount of alkali cation due to a better organization of geopolymer network.

XRD analysis was also performed on the hardened materials (Fig. 4). All the samples showed anorthite, augite, forsterite, magnetite and hematite derived from original precursors (V and G) and quartz and anatase from metakaolin (M). However, in Na/K-VM-20 samples, anorthite and forsterite peaks showed lower intensity in comparison with raw material patterns, demonstrating a partial dissolution due to polycondensation reaction regardless of the alkaline solution used (Fig. 4) and revealing the low reactivity of volcanic materials in alkaline environment [8]. On the contrary in GM-20, a slight difference of intensity of anorthite peaks among Na and K samples were observed, highlighting a higher dissolution in K-GM-20 (Fig. 4) than in the Na-ones. Finally, these intensity modifications in comparison with volcanic raw materials can be

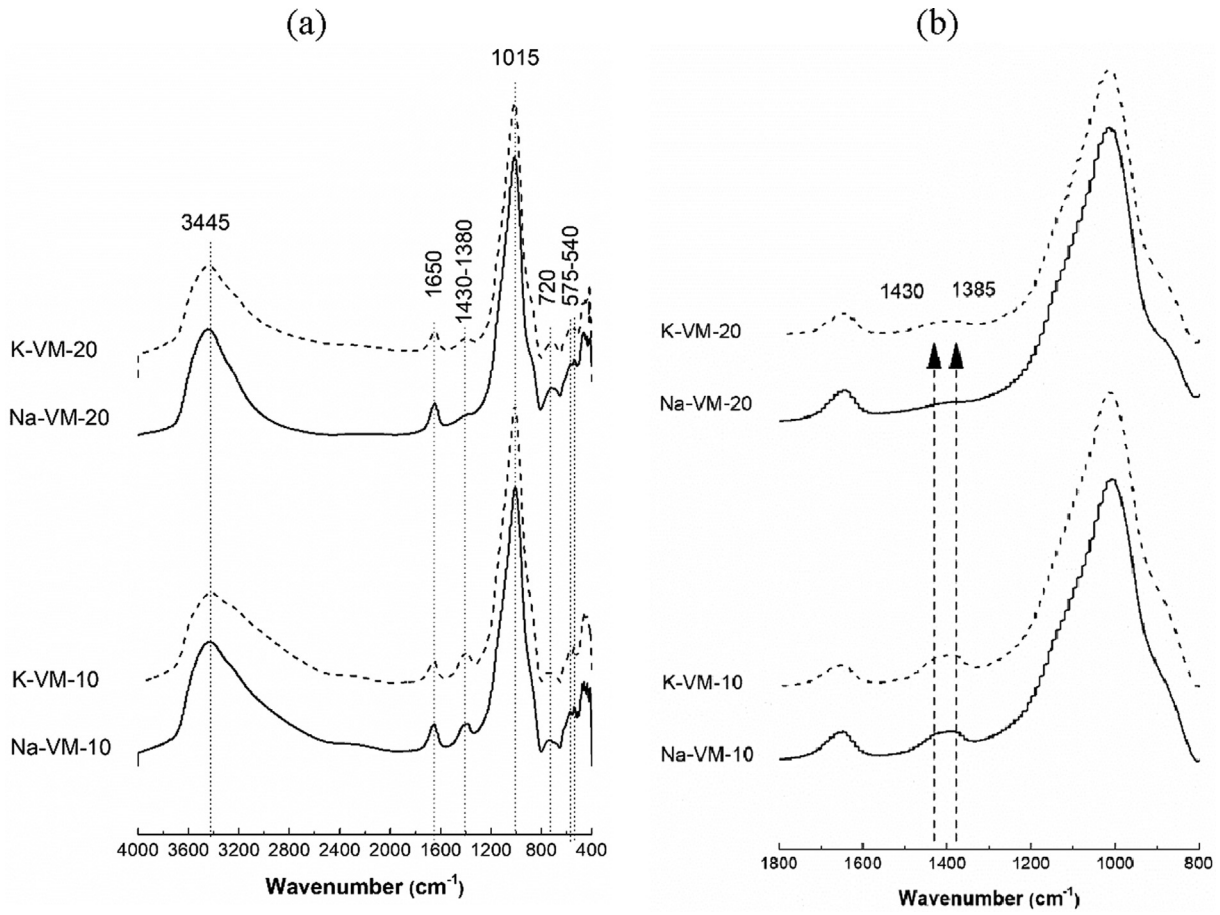

Fig. 3. (a-b) – a) FT-IR spectra obtained using KBr method collected in the range of 4000–400 cm^{-1} for (—) K-VM and (—) Na-VM; b) in the range of 1800–800 cm^{-1}. The dashed arrows indicate the carbonate contributions.

associated to metakaolin contribution which induces the increase of the Si and Al species available, thereby favoring dissolution and network formation [33,34].

3.3.2. Thermal analysis

Thermal analysis was performed on all VM and GM samples to compare the effect of the activating solutions on the thermal stability of the consolidated materials. Fig. 5 shows the thermal behavior of GM-10 samples (selected as representative sample), activated respectively by Na (Fig. 5 a) and K (Fig. 5 b) solutions. Regardless alkaline solution used, the major weight loss of 4.9% is observed below 200 °C and reveals the water of the geopolymer samples [21]. Moreover, the remaining weight loss recorded at higher temperature (200–500 °C) is minimal attesting below 1% related to the release of silicate or aluminate hydroxyl groups as in all materials [21]. Furthermore, the heat flow profiles show a large endothermic peak from 25 to 125 °C, corresponding to water, which appears to be controlled by the alkaline solutions used. Indeed, the thermal curve of sample Na-GM-10 (Fig. 5a) shows a splitting of the large endothermic peak into two smaller ones (~30 and 70 °C), slowly differently from sample K-GM-10, whose endothermic peak is centered around 50 °C (Fig. 5b). The small difference is only due to the intensity of the both contribution corresponding to physical water's loss indicates that there are two type of evaporation process: one of the water molecules evaporating from the pores in the proximity of the particle surface (peak at 30 °C), and one due to the evaporation of water entrapped pores (peak at about 70 °C). Porosity in NaOH/Na silicate activated geopolymers seems to be finer than in the KOH/K silicate activated ones due to the difficulties of water to leave the pores. Further explanation in the paragraphs reporting porosity measurements (Table 5 and Fig. 8). All TGA results are reported in Table 3. Generally, in the low temperature range (25–200 °C), the samples activated by the potassium solution have evidenced a lower weight loss than those activated by sodium solution, except for Na-VM-20, which have showed a contrary tendency. Instead, GM-10 samples evidenced the same values irrespective of the alkaline solutions. These results correlated well with those obtained from FT-IR. The higher the reticulation degree, the lower amount of water is found in the geopolymeric network. In details, the weight loss recorded below 120–150 °C is due to the water content located in the porosity of the samples where are entrapped few H_2O molecules produced during the polycondensation step of the geopolymerization reaction. Such progressive release of water molecules was observed with in situ FTIR analysis during the induration of the fresh pastes. No relation between water and amorphous network was observed with XRD analysis since no hydrated phases were detected. In addition, the TGA results did not show dihydroxylation phenomenon occurring generally from 300 to 800 °C (temperature range for the study of residual polycondensation) [35], demonstrating the stability of the aluminosilicate network and OH– groups already condensed.

3.3.3. Mechanical properties

The stress/strain (σ/ε) curves of all samples after 7 and 21 curing days were plotted in Fig. 6. In general, the metakaolin addition strongly influenced the final mechanical properties such as to observe a considerable increasing of strengths in both VM-20 and

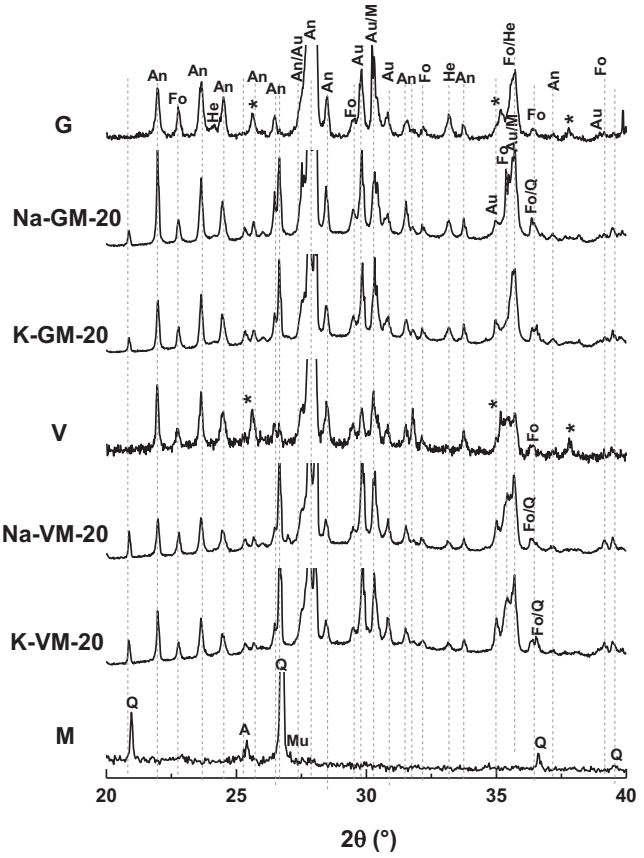

Fig. 4. XRD patterns of raw precursors and consolidated materials. Pdf files: Q: quartz (04-016-2085); An: anorthite (04-05-4988); Au: augite (04-017-4396); Fo: forsterite (04-017-0663); M: Magnetite (00-900-5814) Mu: muscovite (00-060-1516); He: hematite (00-024-0072); A: anatase (00-021-1272), * corundum.

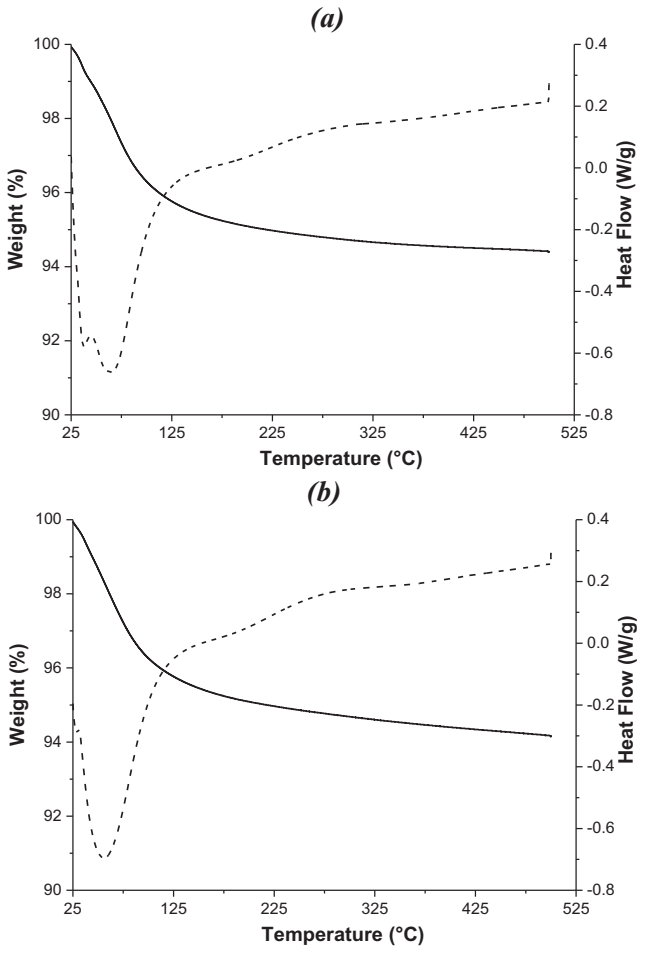

Fig. 5. Thermal curves of weight loss (—) and (—) heat flow for (a) Na-GM-10 and (b) K-GM-10 samples.

GM-20 samples. During mechanical test procedure, the geometrical determination of the apparent density was required, and its values after 7 and 21 curing days, as well as the compressive strength values given by the average of the best 4 values recorded per each formulation with a variability attesting around 5% were reported in Table 4. All samples showed apparent density values ranging between 2.1 and 2.2 g/cm^3 with K-activated samples reporting slightly higher one (Table 4).

The sodium samples (Fig. 6A) evidenced the lowest strengths in comparison with the potassium ones. The higher value after 7 aging days of samples belonging to Na-VM formulation (Fig. 6 Aa), was reached by Na-VM-20 (44 MPa), contrary to 17 MPa recorded for Na-VM-10. Analogously, the samples aged 21 days showed the same behavior: 50 and 18 MPa respectively for Na-VM-20 and Na-VM-10. Similar values were obtained by Na-GM formulation (Fig. 6 Ab), whose values reached respectively 46 and 16 MPa after 7 days and 51 and 17 MPa after 21 days, respectively for Na-GM-20 and Na-GM-10. The compressive strengths values after 21 days find corresponding feedback in literature within the range of 23–60 MPa, depending on alumina available in the geopolymer matrix [27,31,36]. Differently, the potassium samples (Fig. 6B) showed the highest values. Indeed, K-VM samples recorded 23 and 69 MPa after 7 days and 29 and 71 MPa after 21 days, while K-GM samples achieved the highest values of all formulations with 26/78 MPa and 30/89 MPa respectively after 7 and 21 aging days (Fig. 6 Bb). We can deduce that the addition of metakaolin generates a dense composite/mortar where the volcanic ash or ghiara particles act as reactive aggregates. At short aging time (7 days) the strength is not yet developed, indicating the slow reactivity of the volcanic materials with respect to metakaolin that usually completes the reticulation in 7 days for a final strength around 30 MPa [20]. Additionally, even though all samples showed a brittle behavior, there are evidence of a plastic trend, visible as a relevant value of elongation before fracture, in both VM-10 and GM-10 series when activated with sodium (Fig. 6Aa and Ab). This is another indication that the geopolymers with these formulations are not yet completely rigid even after 21 days. Differently from Na activation, K-solution strongly increases elastic modulus and the final mechanical strength (Fig. 6Ba and Bb). When 20 wt% of M is added, the shape of the curves drastically changes and the elongation is strongly reduced.

3.3.4. Porosimetric properties

The comparison of cumulative pore volume trends for each sample taking into account the influence of metakaolin added in the mixture were showed in Fig. 7. Moreover, all porosimetric values obtained by Hg porosimetry analysis, including accessible porosity and cumulative pore volume values in the specific ranges considered were summarized in Table 5. In detail, Na-VM recorded a higher pore volume in the range 1–0.1 μm (2.61 cm^3/g) and 0.1–0.01 μm (59.26 cm^3/g), respectively in VM-10 and VM-20 samples (Fig. 7 Aa) with quite equivalent accessible porosity (~25%) and bulk density (1.9 g/cm^3; Table 5). Instead, K-VM evidenced a higher cumulative pore volume in the large range 1–0.01 μm (18.06 cm^3/g) in VM-20, while the main pore volume for VM-10 was recorded in the smallest range 0.01–0.001 μm (6.36 cm^3/g) (Fig. 7 Ba),

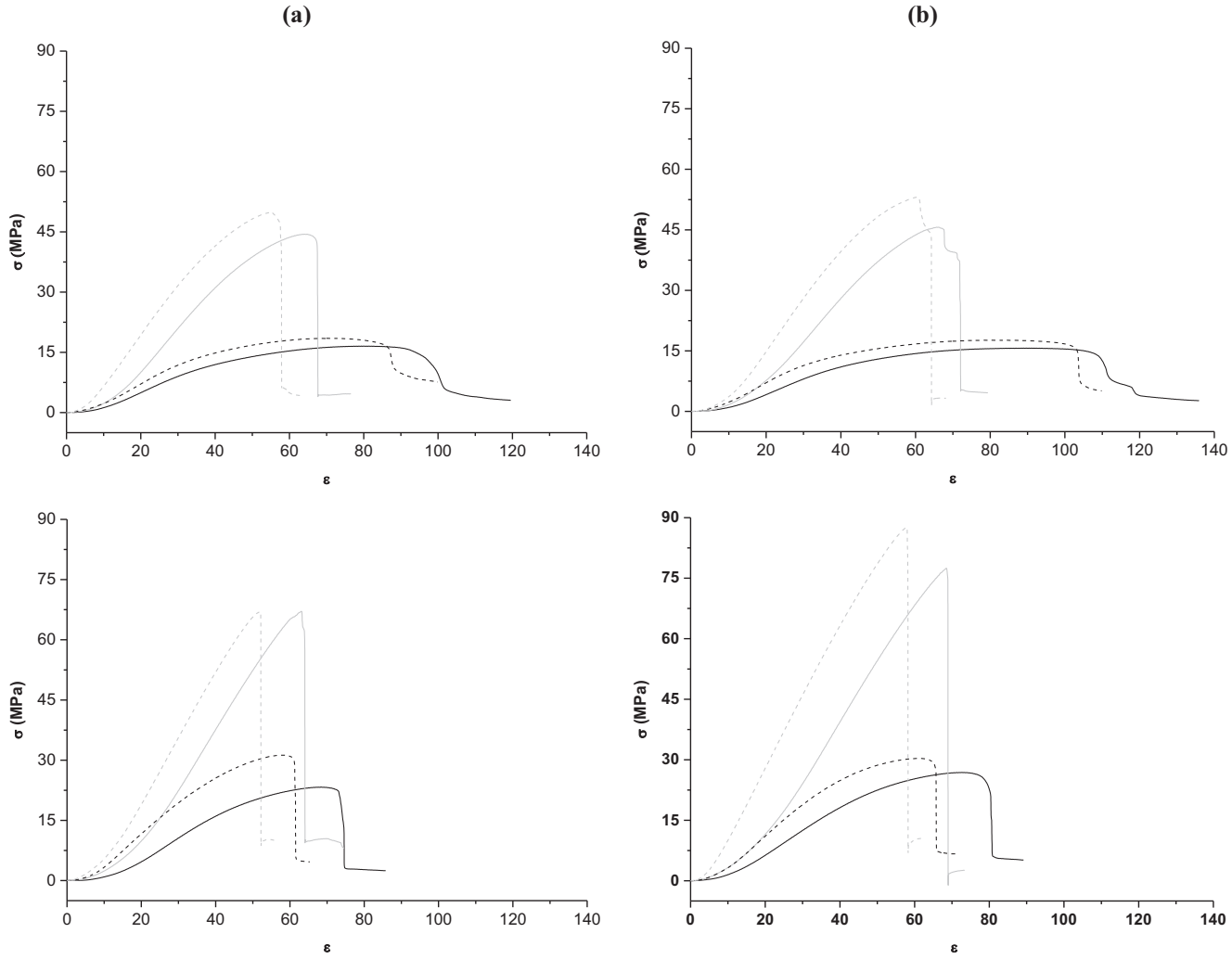

Fig. 6. Average of compressive strength in function of time after (—)7 and (–) 21 days for samples based on (a) VM and (b) GM activated with (A) sodium and (B) potassium solution and with (—) 10 and (—) 20% of metakaolin.

demonstrating its low accessible porosity attesting around 15% contrary to a higher bulk density (2.1 g/cm^3) (Table 5). The Na-GM samples showed the same trends of Na-VM. Indeed, higher cumulative pore volume in 1–0.1 μm range (12.58 cm^3/g) for GM-10, while 12.58 cm^3/g in the 0.1–0.01 range for GM-20 (Fig. 7 Ab). Moreover, slight difference in terms of accessible porosity (±1) and bulk density (±0.1) were recorded (Table 5). K-GM showed a lower porosity (12%) and higher density (2.1 g/cm^3) in GM-10 than GM-20′s features (Table. 5), in addition to higher pore concentration in the bigger range 100–1 μm (0.22 cm^3/g) differently to 24.05 cm^3/g in 0.1–0.001 μm range (Fig. 7 Bb). Therefore, the potassium-samples (K-VM and K-GM) evidenced, generally, higher density and lower accessible porosity with a general decreasing of bigger pore volume than those of sodium one, as also reported by [37]. The porosity values of Na-samples are in accordance to values found in literature [11] as well as the density [38]. Moreover, the influence of metakaolin is better highlighted in potassium samples, which recorded a lower porosity in VM-10 and GM-10 than those with higher metakaolin.

3.3.5. Physical properties correlations

From FTIR data, it was evidenced that the formation of a reticulated network in sodium and potassium with the presence of some carbonate species in both series (Na/K-VM/GM), decreases at increasing M content. Indeed, the mechanical compressive results evidenced some differences among the two activators used. In detail, the samples activated by potassium solution recorded the higher values than those with the sodium, with an increase estimated about 50–60%. Furthermore, an increase of strength for the samples with 20% of M, reached an increase of about 200%. The compressive strengths showed a slight variation, of about 15%, between the values obtained by the test at 7 and 21 days of curing. Moreover, taking into account the average density of each formulation's set and the concentration of alumina in the matrix, progressive linear trends, more evident for the AAMs based on volcanic ash than those one with ghiara were highlighted in Fig. 8. Therefore, the direct proportionality among the concentration of alumina of the precursors and the final compressive resistance was demonstrated.

To obtain an overview on physical properties measured with different methods (apparent density, weight loss, compressive strength and accessible porosity) and to compare the behaviour of the two alkaline solutions used (not focusing on M content), we proposed a matrix scatter plot with the boxplot of variables set in the diagonal to enclose all values measured for easily sum-up (Fig. 9). Indeed, considering the diagrams IIc and IIIb of Fig. 9, a direct correlation between the weight loss [200–500 °C] and the compressive stress values after 7 days can be observed. The

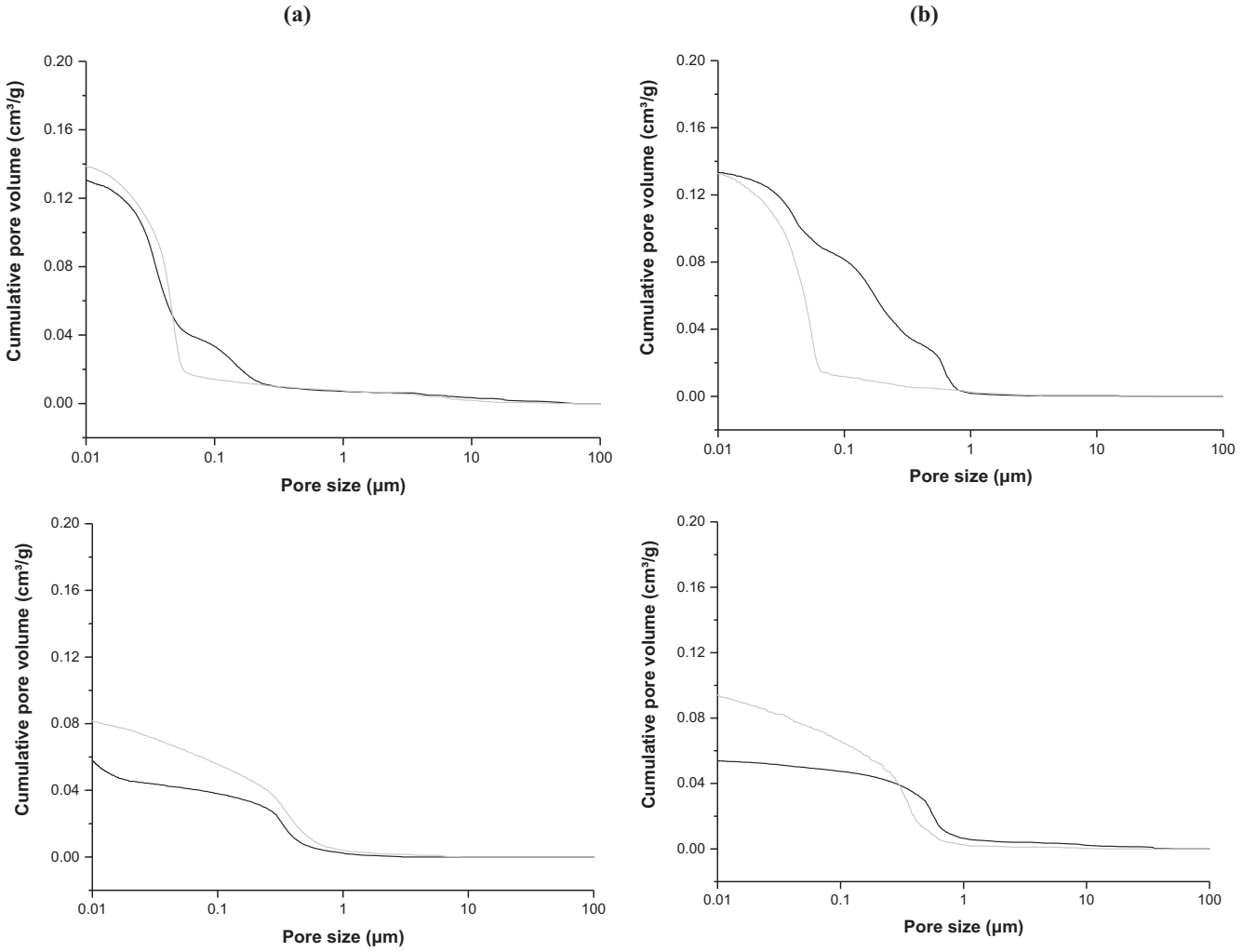

Fig. 7. Cumulative pore volume in function of pore size graphs for samples with (—) 10% and (—) 20% of metakaolin based with (a) VM and (b) GM samples activated with (A) sodium and (B) potassium solution.

Table 5
Density, porosity and pore information obtained by Hg porosimetry analysis for each samples and summary results.

		VM				GM			
		10		20		10		20	
		Na	K	Na	K	Na	K	Na	K
Bulk density (g/cm^3)		1.9	2.1	1.9	1.9	1.9	2.1	1.8	1.9
Accessible porosity (%)		25	15	26	26	25	12	24	19
Total pore volume (cm^3/g)		0.13	0.07	0.14	0.08	0.13	0.05	0.13	0.10
Average pore diameter (μm)		0.04	0.03	0.04	0.06	0.07	0.12	0.04	0.05
∑ incremental volume (cm^3/g) in the following ranges:	100–10 μm	0.04	0.00	0.02	0.00	0.00	0.03	0.00	0.00
	10–1 μm	0.17	0.01	0.19	0.04	0.01	0.19	0.01	0.03
	1–0.1 μm	2.61	3.29	0.48	5.65	12.58	6.75	0.18	8.48
	0.1–0.01 μm	45.19	8.28	59.26	12.41	31.09	6.75	28.45	17.41
	0.01–0.001 μm	7.53	6.36	7.11	4.73	6.56	2.83	6.82	6.64

potassium samples with higher M content show higher weight loss differently to sodium samples with lower M amount. Moreover, there is a relation between apparent density and weight loss for all the samples, the lower the density, the higher the weight loss (Fig. 9, see the box Ic and IIIa), in addition to a clear distribution of Na and K-samples represented by two parallel trends. Finally, an inverse correlation between apparent density, geometrically determined, and accessible porosity, as measured by the Hg-intrusion porosimetry (Fig. 9, see the box IVa and Id) was found indicating the validity of our measurements and a clear polymerization degree, more evident for Na-samples.

4. Conclusion

This paper illustrated the results of polycondensation reactions monitoring of AAMs considered, making a comparison of Na and K solutions in terms of networks, mechanical strengths and porosity. The main conclusions drawn are the following:

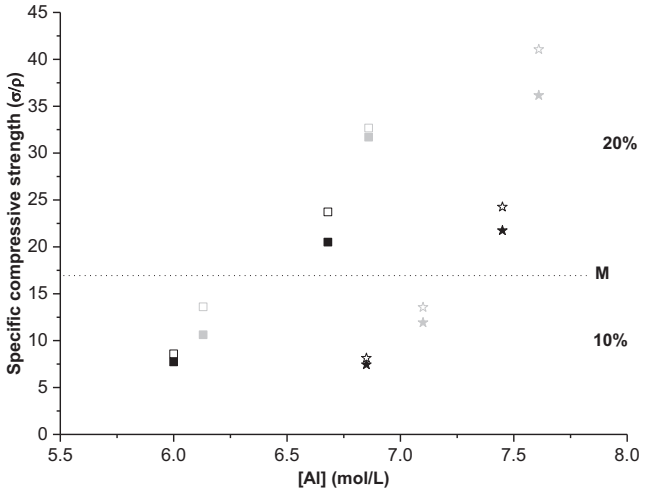

Fig. 8. Value of specific mechanical compressive in function of Al concentration for (■) VM and (★) GM samples with (—) Na and (—) K solution at (■) 7 and (□) 21 days.

- The continuous and progressive shift of the Si-O-M band position (in situ FTIR) in time toward lower wavenumbers confirmed the occurrence of polycondensation reactions regardless of activating solutions used.
- The presence of some carbonate species, starting already in few hours, decreased with higher metakaolin content, as well as potassium samples have evidenced a higher effect regardless the volcanic precursors used.
- The metakaolin contribution favored the partial dissolution of volcanic precursor's mineralogical phases, inducing the increase of the Si and Al species available to create a better network organization. This latter was also confirmed by the low weight loss recorded due to few amounts of free water in the structure.
- The compressive strengths were positively influenced by Al species presented in the matrix thanks to metakaolin amount used, as well as potassium solution enhanced the mechanical properties. Indeed, potassium samples recorded a higher density combined to a lower porosity differently to sodium samples.

Therefore, this work evidenced the possibility to valorise the volcanic deposits of Mt. Etna area in alkaline environment, whose binders can be applied in the local Cultural Heritage restoration preserving the authenticity of substrate in terms of chromatic and chemical-physical aspects [39]. Moreover, their future and potential application will be anticipated by experimental test to evaluate the effects on substrate and immediately after the restoration. The development of these binders, whose precursor is a natural waste material as volcanic ash, represents an important opportunity for all volcanic areas in the world.

CRediT authorship contribution statement

Claudio Finocchiaro: Conceptualization, Investigation, Writing - original draft, Writing - review & editing, Visualization. **Germana Barone:** Conceptualization, Methodology, Resources, Writing - review & editing, Project administration, Funding acquisition, Supervision. **Paolo Mazzoleni:** Conceptualization, Methodology, Writing - review & editing, Supervision. **Cristina Leonelli:** Conceptualization, Methodology, Writing - review & editing, Supervision. **Ameni Gharzouni:** Conceptualization, Data curation, Writing - original draft, Visualization. **Sylvie Rossignol:** Conceptualization, Methodology, Writing - original draft, Supervision.

Declaration of Competing Interest

The authors declare that they have no known competing financial interests or personal relationships that could have appeared to influence the work reported in this paper.

Acknowledgements

This research is supported by the Advanced Green Materials for Cultural Heritage (AGM for CuHe) project (PNR fund with code: ARS01_00697; CUP E66C18000380005).

Appendix A. Supplementary data

Supplementary data to this article can be found online at https://doi.org/10.1016/j.conbuildmat.2020.120095.

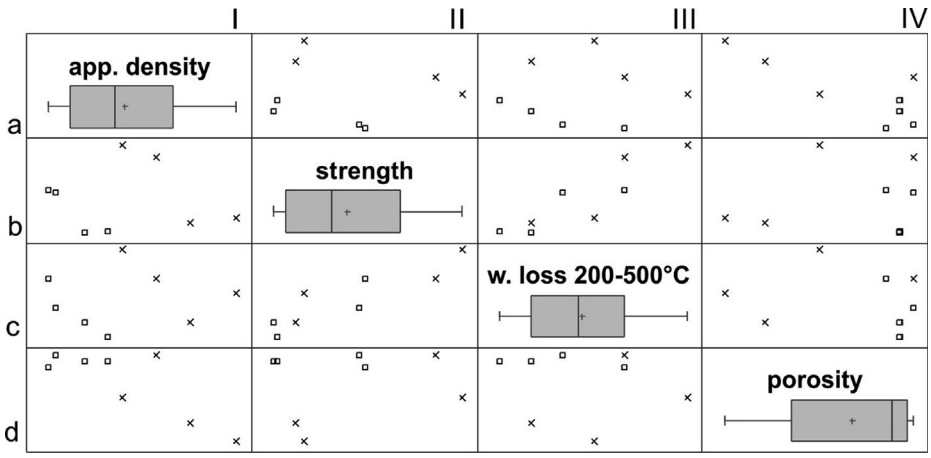

Fig. 9. Matrix scatter plot of density, mechanical strengths after 7 days, weight loss in the range 200–500 °C and accessible porosity; (□) Na and (x) K solutions; Sequences: I-IV for columns; a-d for rows. The boxplots of each variable are reported in the matrix diagonal. The other elements of the matrix are formed by scatter plots of the variable defined by the intersection with the diagonal.

References

[1] Y. Liu, C. Shi, Z. Zhang, N. Li, An overview on the reuse of waste glasses in alkali-activated materials, Resour. Conserv. Recycl. 144 (2019) 297–309, https://doi.org/10.1016/j.resconrec.2019.02.007.

[2] E.A. Obonyo, E. Kamseu, P.N. Lemougna, A.B. Tchamba, U.C. Melo, C. Leonelli, A sustainable approach for the geopolymerization of natural iron-rich aluminosilicate materials, Sustain. 6 (2014) 5535–5553, https://doi.org/10.3390/su6095535.

[3] K.A. Komnitsas, Potential of geopolymer technology towards green buildings and sustainable cities, Procedia Eng. 21 (2011) 1023–1032, https://doi.org/10.1016/j.proeng.2011.11.2108.

[4] P. Duxson, A. Fernández-Jiménez, J.L. Provis, G.C. Lukey, A. Palomo, J.S.J. Van Deventer, Geopolymer technology: the current state of the art, J. Mater. Sci. 42 (2007) 2917–2933, https://doi.org/10.1007/s10853-006-0637-z.

[5] J. Davidovits, Geopolymer, in: Geopolymer Chem. Appl. fourth ed., 2015, pp. 1–37.

[6] J.L. Provis, J.S.J. Van Deventer, Geopolymers: Structure, Processing, Properties and Industrial Applications, Woodhead, 2009.

[7] H.K. Tchakoute, A. Elimbi, E. Yanne, C.N. Djangang, Utilization of volcanic ashes for the production of geopolymers cured at ambient temperature, Cem. Concr. Compos. 38 (2013) 75–81, https://doi.org/10.1016/j.cemconcomp.2013.03.010.

[8] J.N.Y. Djobo, A. Elimbi, H.K. Tchakouté, S. Kumar, Volcanic ash-based geopolymer cements/concretes: the current state of the art and perspectives, Environ. Sci. Pollut. Res. 24 (2017) 4433–4446, https://doi.org/10.1007/s11356-016-8230-8.

[9] P.N. Lemougna, K. tuo Wang, Q. Tang, A.N. Nzeukou, N. Billong, U.C. Melo, X. min Cui, Review on the use of volcanic ashes for engineering applications, Resour. Conserv. Recycl. 137 (2018) 177–190. doi:10.1016/j.resconrec.2018.05.031.

[10] E. Kamseu, C. Leonelli, D.S. Perera, Investigation of volcanic ash based geopolymers as potential, Build. Mater. (2009).

[11] G. Barone, C. Finocchiaro, I. Lancellotti, C. Leonelli, P. Mazzoleni, C. Sgarlata, A. Stroscio, Potentiality of the use of pyroclastic volcanic residues in the production of alkali activated material, Waste Biomass Valorization (2020), https://doi.org/10.1007/s12649-020-01004-6.

[12] L. Contrafatto, Recycled Etna volcanic ash for cement, mortar and concrete manufacturing, Constr. Build. Mater. 151 (2017) 704–713, https://doi.org/10.1016/j.conbuildmat.2017.06.125.

[13] G. Barone, P. Mazzoleni, R.A. Corsaro, P. Costagliola, F. Di Benedetto, E. Ciliberto, D. Gimeno, C. Bongiorno, C. Spinella, Nanoscale surface modification of Mt. Etna volcanic ashes, Geochim. Cosmochim. Acta. 174 (2016) 70–84, https://doi.org/10.1016/j.gca.2015.11.011.

[14] G. Battiato, Le malte del centro storico di Catania, Doc. Dell'Istituto Dipartimentale Di Archit. e Urban. Dell'Università Di Catania, 16 (1988) 85–107.

[15] C.M. Belfiore, M.F. La, M. Viccaro, Technological study of "' ghiara "' mortars from the historical city centre of Catania (Eastern Sicily, Italy) and petro-chemical characterisation of raw materials, (2010) 995–1003. doi:10.1007/s12665-009-0418-5.

[16] G. Bultrini, I. Fragala, G.M. Ingo, G. Lanza, Minero-petrographic, thermal and microchemical investigation of historical mortars used in Catania (Sicily) during the XVII century A.D., Appl. Phys. A 83 (4) (2006) 529–536, https://doi.org/10.1007/s00339-006-3551-y.

[17] L. de Ferri, C. Santagati, M. Catinoto, E. Tesser, E.M. di San Lio, G. Pojana, A multi-technique characterization study of building materials from the Exedra of S. Nicolò l'Arena in Catania (Italy), J. Build. Eng. 23 (2019) 377–387, https://doi.org/10.1016/j.jobe.2019.01.028.

[18] P. Mazzoleni, The use of volcanic stone in architecture: example of Etnean region, Acta Vulcanol. 18 (2007) 141–144.

[19] C. Sciuto Patti, Sui materiali da costruzioni più usati in Catania, Tipografia Editrice dell'Etna, Catania, 1896.

[20] A. Gharzouni, E. Joussein, B. Samet, S. Baklouti, S. Pronier, I. Sobrados, J. Sanz, S. Rossignol, The effect of an activation solution with siliceous species on the chemical reactivity and mechanical properties of geopolymers, J. Sol-Gel Sci. Technol. 73 (2014) 250–259, https://doi.org/10.1007/s10971-014-3524-0.

[21] A. Gharzouni, E. Joussein, B. Samet, S. Baklouti, S. Rossignol, Effect of the reactivity of alkaline solution and metakaolin on geopolymer formation, J. Non. Cryst. Solids. 410 (2015) 127–134, https://doi.org/10.1016/j.jnoncrysol.2014.12.021.

[22] A. Gharzouni, B. Samet, S. Baklouti, E. Joussein, S. Rossignol, Addition of low reactive clay into metakaolin-based geopolymer formulation: synthesis, existence domains and properties, Powder Technol. 288 (2016) 212–220, https://doi.org/10.1016/j.powtec.2015.11.012.

[23] S. Alraddadi, Surface and thermal properties of fine black and white volcanic ash, Mater. Today Proc. (2020), https://doi.org/10.1016/j.matpr.2020.02.429.

[24] J.N.Y. Djobo, A. Elimbi, H.K. Tchakouté, S. Kumar, Reactivity of volcanic ash in alkaline medium, microstructural and strength characteristics of resulting geopolymers under different synthesis conditions, J. Mater. Sci. 51 (2016) 10301–10317, https://doi.org/10.1007/s10853-016-0257-1.

[25] A. Autef, E. Prud'Homme, E. Joussein, G. Gasgnier, S. Pronier, S. Rossignol, Evidence of a gel in geopolymer compounds from pure metakaolin, J. Sol-Gel Sci. Technol. 67 (2013) 534–544. doi:10.1007/s10971-013-3111-9.

[26] L.N. Tchadjié, J.N.Y. Djobo, N. Ranjbar, H.K. Tchakouté, B.B.D. Kenne, A. Elimbi, D. Njopwouo, Potential of using granite waste as raw material for geopolymer synthesis, Ceram. Int. 42 (2016) 3046–3055, https://doi.org/10.1016/j.ceramint.2015.10.091.

[27] R.A. Robayo-salazar, R. Mejía, D. Gutiérrez, F. Puertas, Effect of metakaolin on natural volcanic pozzolan-based geopolymer cement, Appl. Clay Sci. 132–133 (2016) 491–497, https://doi.org/10.1016/j.clay.2016.07.020.

[28] S.A. Bernal, R.M. de Gutierrez, J.L. Provis, V. Rose, Effect of silicate modulus and metakaolin incorporation on the carbonation of alkali silicate-activated slags, Cem. Concr. Res. 40 (2010) 898–907, https://doi.org/10.1016/j.cemconres.2010.02.003.

[29] M. Cyr, R. Pouhet, Carbonation in the pore solution of metakaolin-based geopolymer, Cem. Concr. Res. 88 (2016) 227–235, https://doi.org/10.1016/j.cemconres.2016.05.008.

[30] C. Dupuy, A. Gharzouni, I. Sobrados, N. Tessier-Doyen, N. Texier-Mandoki, X. Bourbon, S. Rossignol, Formulation of an alkali-activated grout based on Callovo-Oxfordian argillite for an application in geological radioactive waste disposal, Constr. Build. Mater. 232 (2020), https://doi.org/10.1016/j.conbuildmat.2019.117170 117170.

[31] H.T. Kouamo, A. Elimbi, J.A. Mbey, C.J.N. Sabouang, D. Njopwouo, The effect of adding alumina-oxide to metakaolin and volcanic ash on geopolymer products: a comparative study, Constr. Build. Mater. 35 (2012) 960–969, https://doi.org/10.1016/j.conbuildmat.2012.04.023.

[32] X.X. Gao, P. Michaud, E. Joussein, S. Rossignol, Behavior of metakaolin-based potassium geopolymers in acidic solutions, J. Non. Cryst. Solids. 380 (2013) 95–102, https://doi.org/10.1016/j.jnoncrysol.2013.09.002.

[33] A. Hajimohammadi, J.L. Provis, J.S.J. Van Deventer, The effect of silica availability on the mechanism of geopolymerisation, Cem. Concr. Res. 41 (2011) 210–216, https://doi.org/10.1016/j.cemconres.2011.02.001.

[34] C. Ruiz-Santaquiteria, A. Fernández-Jiménez, J. Skibsted, A. Palomo, Clay reactivity: production of alkali activated cements, Appl. Clay Sci. 73 (2013) 11–16, https://doi.org/10.1016/j.clay.2012.10.012.

[35] P. Duxson, G.C. Lukey, J.S.J. Van Deventer, Physical evolution of Na-geopolymer derived from metakaolin up to 1000 °c, J. Mater. Sci. 42 (2007) 3044–3054, https://doi.org/10.1007/s10853-006-0535-4.

[36] H. Tchakoute Kouamo, J.A. Mbey, A. Elimbi, B.B. Kenne Diffo, D. Njopwouo, Synthesis of volcanic ash-based geopolymer mortars by fusion method: effects of adding metakaolin to fused volcanic ash, Ceram. Int. 39 (2013) 1613–1621, https://doi.org/10.1016/j.ceramint.2012.08.003.

[37] A. Gharzouni, I. Sobrados, E. Joussein, S. Baklouti, S. Rossignol, Predictive tools to control the structure and the properties of metakaolin based geopolymer materials, Colloids Surfaces A Physicochem. Eng. Asp. 511 (2016) 212–221, https://doi.org/10.1016/j.colsurfa.2016.09.089.

[38] P.N. Lemougna, K.J.D. Mackenzie, U.F.C. Melo, Synthesis and thermal properties of inorganic polymers (geopolymers) for structural and refractory applications from volcanic ash, 37 (2011) 3011–3018. doi:10.1016/j.ceramint.2011.05.002.

[39] ISCARSAH, Principles for the Analysis, Conservation and Structural Restoration of Architectural Heritage, Int. Counc. Monum. Sites. (2003) 3–6.